30518 to Dr. Barry Honig, whom I thank for support and stimulating discussions.

References

Lee, B., & Richards, F. (1971) *J. Mol. Biol. 55*, 379–400.
Rashin, A. A. (1979) *Stud. Biophys. 77*, 177–184.
Rashin, A. A. (1981) *Nature (London) 291*, 85–87.
Rashin, A. A. (1984) *Biopolymers 23*, 1605–1620.
Titani, K., Hermodson, M. A., Ericsson, L. H., Walsh, K. A., & Neurath, H. (1972) *Biochemistry 11*, 2427–2435.
Vita, C., Fontana, A., Seeman, J. R., & Chaiken, I. M. (1979) *Biochemistry 18*, 3023–3031.

CO Bond Angle Changes in Photolysis of Carboxymyoglobin†

L. Powers,* J. L. Sessler, G. L. Woolery, and B. Chance

ABSTRACT: Previous studies [Chance, B., Fischetti, B., & Powers, L. (1983) *Biochemistry 22*, 3820–3829] of the local structure changes around the iron in carboxymyoglobin on photolysis at 4 K revealed that the iron–carbon distance increased ~0.05 Å but was accompanied by a lengthening of the iron–pyrrole nitrogen bonds of the heme (~0.03 Å) that was not as large as that found in the deoxy form. Further analysis of these data together with comparison to model compounds indicates that the Fe–C–O bond angle in carboxymyoglobin is bent (127 ± 4°), having a structure identical, within the error, with the "pocket" porphyrin model compound FePocPiv(1-MeIm)(CO) [Collman, J. P., Brauman, J. I., Collins, T. J., Iverson, B. L., Lang, G., Pettman, R., Sessler, J. L., & Walters, M. A. (1983) *J. Am. Chem Soc. 105*, 3038–3052]. On photolysis, this angle decreases by 5–10°. In addition, correlation is observed between the increase in the length of the Fe–C bond and the decrease of the Fe–C–O angle. These results suggest that the rate-limiting step in recombination is the thermal motion of CO in the pocket to achieve an appropriate bonding angle with respect to the iron. These changes constitute the first molecular picture of the photolysis process, as well as the structure of the geminate state, and are important in clarifying nuclear tunneling parameters.

The photolysis and recombination of carboxymyoglobin at 4 K have been shown to involve a displacement of the CO by ~0.05 Å accompanied by expansion of the iron–pyrrole nitrogen bonds of the heme (Fe–N_p) of ~0.03 Å and possibly lengthening of the iron–proximal histidine (Fe–N_ϵ) bond by ~0.02 Å (Chance et al., 1983). This Fe–N_p average distance is less than that observed for deoxymyoglobin (Mb) with the Fe–N_ϵ distance ~0.10 Å longer (Chance et al., 1983; Takano, 1977). Thus, the structure of this geminate-state photoproduct (Mb*CO) differs significantly from that of Mb. Whatever the molecular origin of this difference, the motion of the CO in recombination to form MbCO must be a step of low activation energy (Austin et al., 1975), producing a small change in the charge density of the iron and a small change in the Fe–C distance (Chance et al., 1983). Rotation of the CO from a preferred position was suggested by Hush (Grady, et al., 1978) from octapole moment studies of CO compounds and by Alben et al. (1983) from studies of the CO stretching frequencies. The possibility that an Fe–C–O bond angle change occurs on photolysis, which may provide the rate-limiting step in recombination, has not been considered.

Although crystallographic studies of small molecules and models having terminal CO groups show the Fe–C–O bond to be nearly linear (Peng & Ibers, 1976; Hoard, 1975), Fe–C–O angles of 135–145° have been observed in several carboxy hemoproteins, including erythrocruorin (Huber et al., 1970), bloodworm *Glycera dibranchiata* (Padian & Love, 1974), horse hemoglobin (Heidner et al., 1976), and myoglobin (Norvell et al., 1975). Presented here are EXAFS (extended X-ray absorbance fine structure) studies of a variety of model compounds and corresponding proteins at 4 K, which are compared to those of carboxymyoglobin and its photoproduct (Chance et al., 1983). We conclude that carboxymyoglobin has an Fe–C–O bond angle of 127 ± 4° and an identical structure within our error with that of the "pocket" porphyrin model FePocPiv(1-MeIm)(CO) (Collman et al., 1983a). This angle decreases 5–10° on photolysis at 4 K.

Materials and Methods

Sample Preparation, Cryogenic Technique, and Sample Monitoring. $Ni(CO)_4$, $Na_2Fe(CO)_4$, and $Fe(CO)_5$ were purchased commercially at the highest purity available and used without further purification. Fe(TPP)(Py)(CO) was prepared by the method of Peng & Ibers (1976), the "pocket" porphyrin FePocPiv(1-MeIm)(CO) by the method of Collman et al. (1983a), and the "picket fence" porphyrin FeTpivP(1-MeIm)(CO) by the method of Collman et al. (1975). MbO_2, met-Mb, and HbO_2 were prepared by methods similar to those reported for MbCO (Chance et al., 1983). Cryogenic techniques and sample monitoring by optical spectroscopy were identical with those reported in detail for MbCO (Chance et al., 1983).

Data Analysis. Data were analyzed by procedures discussed previously (Powers et al., 1981; Lee et al., 1981; Chance et al., 1983) and included background subtraction of the "isolated atom" contribution and k^3 (wave vector) multiplication followed by Fourier transformation. The respective coordination shell contributions were isolated by Fourier filter and back-transformation.

The filtered data of the first shell contributions were then fit by a two atom type procedure (Lee et al., 1981; Peisach

† From AT&T Bell Laboratories, Murray Hill, New Jersey 07974 (L.P.), Stanford University, Stanford, California 94305 (J.L.S.), Princeton University, Princeton, New Jersey 08544 (G.L.W.), and the Institute for Structural and Functional Studies, University City Science Center, Philadelphia, Pennsylvania 19104 (B.C.). *Received October 26, 1983.* Work done at Stanford University (J.L.S.) was supported by NIH Grant GM17880-14, at Princeton University (G.L.W.) by NIH Grant HL-12526, and at the Institute for Structural and Functional Studies (B.C.) by NIH Grants GM-27308, HL-15061, GM-27476, and GM-28385 and NSF Grant PCM-80-26684.

0006-2960/84/0423-5519$01.50/0

et al., 1982; Chance et al., 1983) with bis(imidazole)($\alpha,\beta,\sigma,\gamma$-tetraphenylporphinato)iron(III) chloride (Im_2FeTPP) (Collins et al., 1972) for Fe–N bonds, Fe^{3+}–acetylacetonate (Iball & Morgan, 1967a,b) for Fe–O bonds or $K_3Fe(CN)_6$ (Figgis et al., 1969) for Fe–C bonds in the same manner described by Chance et al. (1983) for MbCO and Mb*CO. Each atom type in the fitting procedure is represented by an average distance, an amplitude factor containing the number of ligands, a change in Debye–Waller factor with respect to the model compound, and a change in threshold with respect to the model. The latter was always small (≤3 eV) and due to significant correlation between the amplitude factor and the change in Debye–Waller factor (Peisach et al., 1982); the amplitudes were constrained to their known values. Generally, no significant changes were observed in the sum of the residuals squared when these were then allowed to vary.

There are three unresolved contributions (atom types) in the first shell: pyrrole nitrogens from the heme ($Fe–N_p$), proximal nitrogen from the histidine ($Fe–N_\epsilon$), and the carbon from CO (or O from O_2) [Fe–C(O)]. However, these require more parameters for fitting (four each as described above) than the number of degrees of freedom in the data (Lee et al., 1981). Therefore, the two atom type fitting procedure with constrained amplitudes was used to map the solutions in parameter space in the following manner. A constrained amplitude ratio of the two contributions of 4/2 gives the average $Fe–N_p$ distance as one contribution and the average of $Fe–N_\epsilon$ and Fe–C(O) as the other. These averages are, however, $1/r^2$ weighted averages and not true arithmatic averages. Other fits of constrained amplitude ratio of 5/1 average $Fe–N_p$ distances and one axial distance (e.g., $Fe–N_\epsilon$) as one contribution and the other axial distance [e.g., Fe–C(O)] as the other and vice versa. Comparison of these constrained amplitude ratio fits gives solutions for each of the three contributions. This procedure is discussed at length and demonstrated for MbCO and Mb*CO in Chance et al. (1983).

Now that the possible solutions for each contribution have been deduced, it is necessary to determine if these solutions, in combination, are indeed representative of contributions that exist in the data and are not artifacts of the fitting procedures (Lee et al., 1981; Peisach et al., 1982). A highly restricted consistency test was used that allows three atom type contributions but constraints *both* the average distances and the amplitude factors. Thus, all the independent parameters are constrained since change in Debye–Waller is highly correlated to amplitude factor and change in threshold is slightly correlated to the distance. Hence, if the sum of residuals squared in the consistency test is not at least as small as the smallest value obtained in the two atom type procedures with constrained amplitude ratio, then the combination of the three contributions is not a compatible solution. If the sum of residuals squared is as small or smaller, the combination must be iterated to determine if these solutions in fact produce a minimum; i.e., one distance was allowed to vary while its amplitude factor together with the other distances and amplitude factors was constrained. In all cases, the minimum was sharp with respect to the distances, and those obtained by this iterated procedure differed no more than ±0.02 Å from those obtained by the two atom type fitting procedures. These values are shown in Table I and are compared to results from crystallography studies.

The partially resolved second and third shell contributions were Fourier filtered together and fit by using those from the model compound Im_2FeTPP with the amplitude constrained to represent the heme and proximal carbon contributions (8 C at 3.0 Å and 4 C at 3.13 Å). An additional oxygen atom was then introduced with amplitude constrained by a two atom type fitting procedure as described earlier. This method is discussed at length by Spiro et al. (1983) and Woolery et al. (1984), who have demonstrated its capabilities in higher shell analysis of hemocyanin and related compounds that contain unresolved imidazole contributions.

Two model compounds were used to represent the Fe–O contribution: (I) Fe^{3+}–acetylacetonate representing a bent Fe–O configuration having no multiple scattering contributions and (II) $Fe(CO)_5$ (Wyckoff, 1963a) having a linear Fe–O configuration and maximum multiple scattering contribution. It has been shown both experimentally and theoretically that when three atoms are nearly collinear (angle > 140°), the amplitude and phase contributions of the third atom are distorted and comparison with standard analysis procedures yields erroneous results (Lee et al., 1981; Teo, 1981; Co et al., 1983). Comparison of I and II shows an amplitude enhancement of a factor of 2.5 and distance distortion of −0.15 Å for II representing the maximum effects of multiple scattering. Results of this procedure with both I and II for the Fe–O contribution are given in Table II. The error in average distances calculated in this procedure is ±0.02 Å. A survey of various model compounds containing –C–O (Wyckoff, 1963a,b; Peng & Ibers, 1976) showed the C–O bond distance to be 1.15 ± 0.02 Å while that for O–O was 1.22 ± 0.02 Å (Wyckoff, 1963b; Phillips, 1980). The C–O distance for an isolated CO molecule is 1.05 ± 0.02 Å (Wyckoff, 1963b) as is expected for Mb*CO from the infrared measurements of Alben et al. (1980). These were used to calculate the Fe–C–O (or Fe–O–O) bond angles of Table II.

Results

The results of the background-subtracted, k^3-multiplied EXAFS data for MbCO, Mb*CO, and chemically produced Mb are given in Chance et al. (1983). These data for MbO_2, met-Mb, HbO_2, and the porphyrin models are comparable in signal to noise, while those of the other model compounds are a factor of 10 or more better. Figure 1 compares the Fourier transforms of the Mb derivatives. It is clear that there is a similarity between MbO_2 and MbCO, especially in the partially resolved second and third shell. Although analysis of the first shell filtered data of these Mb derivatives (Table I) shows significant differences in the $Fe–N_\epsilon$ and Fe–C (Fe–O) distances, the partially resolved second and third shell contributions are quite similar. The Fe–O–O bond angle in MbO_2 has been determined by crystallography (Phillips, 1980) to be significantly bent at 115 ± 5°, and the similarity with MbCO indicates that the Fe–C–O angle is also bent, in agreement with the 135° value found by neutron diffraction studies (Norvell et al., 1975). Further evidence for a bent Fe–C–O angle is apparent in Figure 2 where MbCO is compared with the open-cavity "picket fence" and encumbered "pocket" models in which linear and bent carbonyl geometries are expected (Collman et al., 1983b). The partially resolved second and third shell contribution in MbCO (and MbO_2) is similar to that of the pocket porphyrin model FePocPiv(1-MeIm)(CO), which incorporates synthetically tailored distal-side steric interactions (Collman et al., 1983a). By contrast, the Fe–C–O angle in the picket fence porphyrin model FeTpivP(1-MeIm)(CO) is similar to the linear arrangement of Fe(TPP)(Py)(CO) and significantly different from MbCO, FePocPiv(1-MeIm)(CO), and MbO_2.

Another similarity is also apparent in Figure 1 between the partially resolved second and third shell contributions of Mb and met-Mb. Mb*CO, however, is somewhat different, having

Table I: First Coordination Shell Distances of Oxygen-Binding Heme Protein Derivatives and Model Compounds

compd	Fe–N_p (Å)		Fe–N_ϵ (Å)		Fe–C(O) (Å)	
	cryst	EXAFS[a]	cryst	EXAFS[a]	cryst	EXAFS[a]
$Ni(CO)_4$[b]					1.84	1.80
$Na_2Fe(CO)_4$[b,c]					1.75	1.75
$Fe(CO)_5$[b]					1.79–1.84	1.82
Fe(TPP)(Py)(CO)[d]	2.02	2.02	2.10	2.09	1.77	1.81
HbO_2	1.99[e]	1.99	2.07[e]	2.05	1.67–1.83[f]	1.82
MbO_2[g]	1.95	2.02	2.07	2.06	1.83	1.80
FePocPiv(1-MeIm)(CO) (pocket model)		2.01		2.23		1.94
FeTpivP(1-MeIm)(CO) (picket fence model)		2.02		2.05		1.80
MbCO[a]		2.01		2.20		1.93
Mb*CO[a]		2.03		2.22		1.97
met-Mb[h]	2.04	2.04	2.13	2.11	2.00	1.88
Mb[i]	2.06	2.06	2.10	2.12		

[a] Distances determined by the procedures given in Chance et al. (1983); error ±0.02 Å. [b] Wyckoff, 1963a,b. [c] Teo, 1981. [d] Peng & Ibers, 1976. [e] EXAFS results; Eisenberger et al., 1978. [f] Shaanan, 1982. [g] Phillips, 1980. [h] Takano, 1977a. [i] Takano, 1977b.

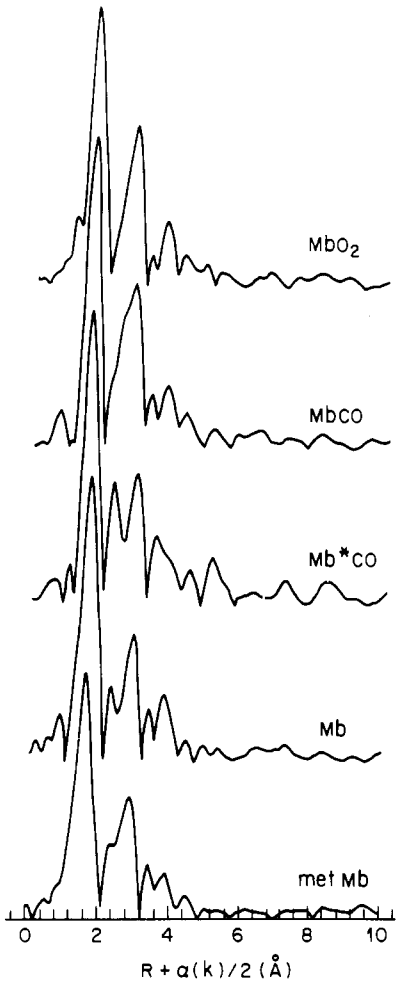

FIGURE 1: Comparison of the Fourier transforms of Fe EXAFS data of myoglobin derivatives after background subtraction and multiplication by k^3. $\alpha(k)$ is the absorber–scatterer phase shift (Powers et al., 1981).

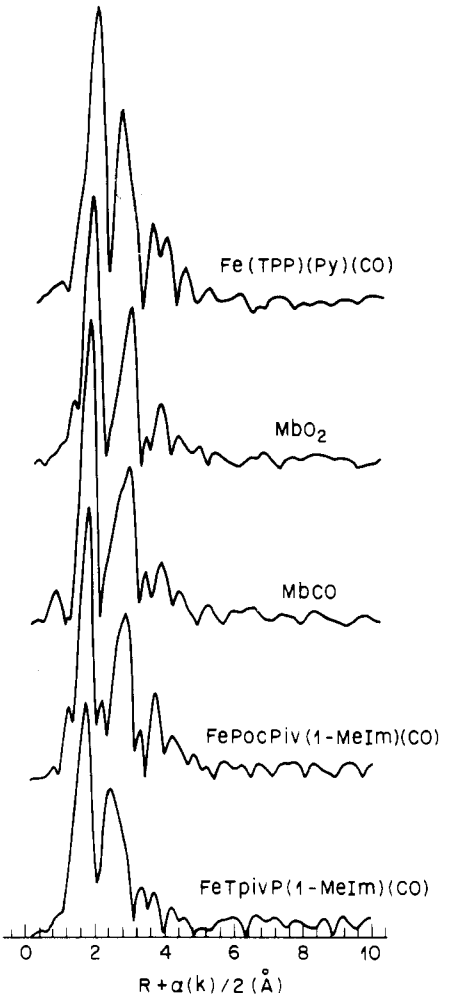

FIGURE 2: Comparison of the Fourier transforms of Fe EXAFS data for the pocket and picket fence model compounds (Collman et al., 1983a, b) with that of myoglobin after background subtraction and k^3 multiplication. $\alpha(k)$ is the absorber–scatterer phase shift (Powers et al., 1981).

a larger contribution in the shorter distance portion. Since Mb and met-Mb have no other contributions than heme and proximal histidine in this region (H's from H_2O are not detected by this technique) and C of CO is observed in the first coordination shell of Mb*CO (Chance et al., 1983; Table I), the difference is likely due to O. Subtraction of this heme and proximal histidine contribution gives a single O contribution at 2.62 ± 0.02 Å.

The results of the two fitting procedures described under Data Analysis are given in Table II.[1] Comparison of these procedures shows that the bent (I) and linear (II) Fe–C–O configurations differ significantly in average distance (~0.15 Å) and in magnitude of the amplitude (~2.5). In addition, little difference in either the average distance or magnitude of the amplitude is found between the bent (I) fit and the

[1] $Ni(CO)_4$ was included as a model for the linear configuration since the core electron properties of Ni are similar to those of Fe and they are difficult to distinguish in the EXAFS analysis.

Table II: Second–Third Coordination Shell Distances of Oxygen-Binding Heme Protein Derivatives and Model Compounds

	X-ray crystallography			EXAFS[a]				
					Fe–O			
					bent (I)		linear (II)	
compd	Fe–C (Å)	Fe–O (Å)	Fe–C(O)–O (deg)	Fe–C (Å)[b]	Fe–O (Å)	Fe–C(O)–O (deg)	Fe–O (Å)	Fe–C(O)–O (deg)
$Ni(CO)_4$[c]		2.99	179		2.82	145 ± 8	2.99	180 ± 11
$Na_2Fe(CO)_4$[c,d]		2.92	177		2.78	146 ± 8	2.93	180 ± 11
$Fe(CO)_5$[c]		2.90–2.99	180		2.81	141 ± 8	2.98	180 ± 11
Fe(TPP)(Py)(CO)[e]	3.18	2.89	179	3.18	2.77	138 ± 6	2.96	180 ± 11
HbO_2[f]		2.91	156	3.07	2.67	122 ± 4	2.89	143 ± 8
MbO_2[g]		2.60	115	3.13	2.69	123 ± 4	2.91	148 ± 8
FePocPiv(1-MeIm)(CO) (pocket model)				3.13	2.79	127 ± 4	2.98	148 ± 8
FeTpivP(1-MeIm)(CO) (picket fence model)				3.14	2.76	137 ± 4	2.94	170 ± 10
MbCO[h]			135	3.14	2.78	127 ± 4	2.95	145 ± 8
Mb*CO				3.16	2.62	117 ± 4	2.81	135 ± 6

[a] Distances determined by procedures under Data Analysis; error ±0.02 Å. [b] Average of heme and proximal histidine contributions consisting of two partially resolved shells; model is Im_2FeTPP with average distance 3.13 Å, see Data Analysis. [c] Wyckoff, 1963a,b. [d] Teo, 1981. [e] Peng & Ibers, 1976. [f] Shaanan, 1982. [g] Phillips, 1980. [h] Norvell et al., 1975.

crystallography values when the angle is $<\sim 130°$. These trends, although not identical with those reported by Teo (1981) and Co et al. (1983) for Fe–O–Fe, are qualitatively similar. The results of either the bent (I) or linear (II) fit agree well with the crystallography data: linear (II) fit for angles $\geq 150°$ and bent (I) fit for angles $\leq 130°$.

When these procedures are used for comparison, MbO_2, MbCO, and FePocPiv(1-MeIm)(CO) are similar, having a Fe–C–O bond angle of $\sim 125°$. [In fact, FePocPiv(1-MeIm)(CO) is identical within the error with MbCO in the first coordination shell fit as well as the higher shells.] The result for Mb*CO is identical with that found earlier by subtraction of the heme and proximal histidine contribution with an Fe–C–O angle of $\sim 117°$. Note that, in each case where the Fe–C–O is bent, the Fe–C and Fe–N_ϵ bond distances (Table I) are ~ 0.13 Å longer than when Fe–C–O is linear.

Thus, it is evident that the Fe–C–O angle has decreased on photolysis since the Fe–C distance increases 0.05 ± 0.03 Å (Chance et al., 1983) and the Fe–O distance decreases 0.16 ± 0.03 Å (Table II). Assuming values for the C–O bond discussed earlier (Data Analysis), the Fe–C–O angle decreases 5–10°.

Discussion

Comparison of the first coordination shell distances found by EXAFS at 4 K with those reported from crystallography studies (Table I) shows good agreement (within the error of the two measurements) and indicates that the local structure of the heme groups is not distorted to any large extent by low temperature. Similarly, comparison of the results of the bent (I) and linear (II) fits and those from crystallography studies (Table II) is also in good agreement, depending on which is applicable to the compound [linear (II) fit for angles $\geq 150°$ and bent (I) fit for angles $\leq 130°$].

Photolysis decreases the molecular orbital overlap further (Walek & Loew, 1982) by decreasing the Fe–C–O angle by 5–10° and is accompanied by lengthening of the Fe–C bond by ~ 0.05 Å, Fe–N_p bonds by ~ 0.03 Å, and, possibly, the Fe–N_ϵ bond by ~ 0.02 Å (Chance et al., 1983). Recombination could be rate limited by the thermal motion of CO: once the angle appropriate for sufficient overlap is achieved through thermal motion of the CO, an electron is donated from the heme system to the Fe–C bond, and the associated heme bonds contract. At higher temperature (~ 10 K or greater), however, thermal motion of the heme coupled to that of the CO may allow the CO to move far enough from the appropriate orientation to produce Mb as well as recombination.

It is interesting to note that distal side steric encumbrance in the model compounds influences the Fe–C–O angle together with the CO and O_2 binding properties. The pocket porphyrin, incorporating distal side steric interaction, has a local structure identical with that of MbCO. This compound has CO and O_2 association and dissociation rates similar to myoglobin and a CO affinity that is substantially lower than the analagous unencumbered, open-cavity, picket fence model in which a linear Fe–C–O arrangement is observed (Collman et al., 1983b). In the pocket porphyrin, the bent arrangement causes the Fe–C (and Fe–N_ϵ) bond(s) to be longer (0.13 Å), providing less molecular overlap than in the linear picket fence case. Not only are the angles for bound CO and O similar but the charge density around the iron in both cases is similar as determined by their edge energies. Apparently, the restriction of CO by the molecular architecture of the pocket causes the CO to behave as a one-electron donor in much the same way as O_2.

Acknowledgments

We thank Professor James P. Collman for helpful discussions and criticism. A portion of this work was done at the Stanford Synchrotron Radiation Laboratory (SSRL). SSRL is supported by NSF Grant DMR 77-27489, in cooperation with the Stanford Linear Accelerator Center and the U.S. Department of Energy.

Registry No. Fe(TPP)(Py)(CO), 53470-09-0; FePocPiv(1-MeIm)(CO), 78694-32-3; FeTPivP(1-MeIm)(CO), 52215-85-7.

References

Alben, J. O., Beece, P., Brown, S. F., Eisenstein, L., Frauenfelder, H., Good, D., Marden, M. C., P. P., Reinisch, L., Reynolds, A. H., & Yue, K. T. (1980) *Phys. Rev. Lett. 44*, 1157–1160.

Austin, R. H., Beeson, K. W., Eisenstein, L., Frauenfelder, H., Gunsalus, I. C., & Marshall, V. P. (1973) *Science (Washington, D.C.) 181*, 541–543.

Chance, B., Fischetti, B., & Powers, L. (1983) *Biochemistry 22*, 3820–3829.

Co, M. S., Hendreckson, W. A., Hodgson, K. O., & Doniach, S. (1983) *J. Am. Chem. Soc. 105*, 1144–1150.

Collins, D. M., Countryman, R., & Hoard, J. L. (1972) *J. Am. Chem. Soc. 94*, 2066–2073.

Collman, J. P., Gagnê, R. R., Reed, C. A., Halbert, T. R., Lang, G., & Robinson, W. T. (1975) *J. Am. Chem. Soc. 97*, 1427–1439.

Collman, J. P., Brauman, J. I., Collins, T. J., Iverson, B. L., Lang, G., Pettman, R., Sessler, J. L., & Walters, M. A. (1983a) *J. Am. Chem. Soc. 105*, 3038–3052.
Collman, J. P., Brauman, J. I., Iverson, B. L., Sessler, J. L., Morris, R. M., & Gibson, Q. (1983b) *J. Am. Chem. Soc. 105*, 3052–3064.
Eisenberger, P., Shulman, R. G., Kincaid, B. K., Brown, G. S., & Ogawa, S. (1978) *Nature (London) 274*, 30–34.
Figgis, B. N., Gerlock, M., & Mason, R. (1969) *Proc. R. Soc. London, Ser. A 309*, 91–118.
Grady, J. E., Bacskay, G. B., & Hush, N. S. (1978) *J. Chem. Soc., Faraday Trans. 2 74*, 1430–1440.
Heidner, E. J., Ladner, R. C., & Perutz, M. F. (1976) *J. Mol. Biol. 104*, 707–722.
Hoard, J. L. (1975) in *Porphyrins and Metalloporphyrins* (Smith, K. M., Ed.) Chapter 8, Elsevier, New York.
Huber, R., Epp, O., & Formanek, H. (1970) *J. Mol. Biol. 52*, 340–354.
Iball, J., & Morgan, C. H. (1970a) *Acta Crystallogr., Sect. B 23*, 239–244.
Iball, J., & Morgan, C. H. (1970b) *Acta Crystallogr., Sect. B 23*, 349–354.
Lee, P. A., Citrin, P. H., Eisenberger, P. M., & Kincaid, B. M. (1981) *Rev. Mod. Phys. 53*, 769–806.
Norvell, J. C., Nunes, A. C., & Schoenborn, B. P. (1975) *Science (Washington, D.C.) 190*, 568–570.
Padian, E. A., & Love, W. E. (1974) *J. Biol. Chem. 249*, 4067–4078.
Peisach, J., Powers, L., Blumberg, W. E., & Chance, B. (1982) *Biophys. J. 38*, 277–285.
Peng, S.-M., & Ibers, J. A. (1976) *J. Am. Chem. Soc. 98*, 8032–8036.
Phillips, S. E. (1980) *J. Mol. Biol. 147*, 531–554.
Powers, L., Chance, B., Ching, Y., & Angiolillo, P. (1981) *Biophys. J. 34*, 465–498.
Shaanan, B. (1982) *Nature (London) 296*, 683–684.
Spiro, T. G., Woolery, G. L., Brown, J. M., Powers, L., Winkler, M. E., & Solomon, E. I. (1983) in *Cooper Coordination Chemistry: Biochemical and Inorganic Perspectives* (Karlin, D., & Zubieta, J., Eds.) pp 23–41, Adenine Press, New York.
Takano, T. (1977a) *J. Mol. Biol. 110*, 537–568.
Takano, T. (1977b) *J. Mol. Biol. 110*, 569–584.
Teo, B. K. (1981) *J. Am. Chem. Soc. 103*, 3990–4001.
Walek, A., & Loew, G. (1982) *J. Am. Chem. Soc. 104*, 2346–2351.
Woolery, G. L., Powers, L., Winkler, M., Solomon, E. I., & Spiro, T. G. (1984) *J. Am. Chem. Soc. 106*, 86–92.
Wyckoff, R. W. G. (1963a) in *Crystal Structures*, 2nd ed., Vol. 2, pp 226–227, 178–179, Interscience, New York.
Wyckoff, R. W. G. (1963b) in *Crystal Structures*, 2nd ed., Vol. 1, pp 185–186, 29–30, Interscience, New York.

Assignment of Resonances in the ^{31}P NMR Spectrum of d(GGAATTCC) by Regiospecific Labeling with Oxygen-17†

B. A. Connolly and F. Eckstein*

ABSTRACT: The chemical synthesis of the octanucleotide d(GGAATTCC) in which each of the phosphate groups is sequentially replaced by an ^{17}O-containing phosphate group using a polymer-supported phosphoramidite method is described. All seven phosphorus resonances in the ^{31}P spectrum of d(GGAATTCC) can be resolved. Assignment of these resonances to a particular phosphate group in the chain is possible because labeling of a phosphate with ^{17}O causes its particular signal to disappear from the spectrum. Phosphate residues toward the middle of the octamer have ^{31}P NMR shifts similar to those found in polydeoxynucleotides, whereas those toward the ends resemble those of dinucleoside phosphates. These data are interpreted in terms of less flexibility of the phosphate groups in the center of the molecule as compared to those at the ends.

X-ray fiber diffraction patterns of DNA and polydeoxynucleotides have shown that these molecules predominantly exist as right-handed helices in two conformations, designated the A and B forms. With the availibility of single crystals of oligodeoxynucleotides, X-ray structural analysis has provided a more detailed picture of the structure and conformation of such oligonucleotides and in particular has revealed the existence of a left-handed helix, designated the Z conformation. The results obtained with oligonucleotides are generally considered representative of the structure of polynucleotides and DNA (Dickerson et al., 1982; Zimmerman & Pheiffer, 1982; Arnott et al., 1983; Saenger, 1983; Wang et al., 1983; Zimmerman, 1983). Most recently, modern NMR spectroscopic techniques have facilitated the assignment of the protons in such oligodeoxynucleotides (Patel et al., 1982a,b, 1983a,b; Kan et al., 1982; Clore & Gronenborn, 1983; Feigon et al., 1983; Hare et al., 1983; Pardi et al., 1983; Scheek et al., 1983). These studies provide information on the conformation of oligonucleotides in solution and thus complement the data obtained by X-ray structural analysis on the conformation in crystals. In contrast to ^{1}H NMR spectroscopy, ^{31}P NMR spectroscopic data although recorded for a number of oligodeoxynucleotides have been less informative, mainly because the signals observed in the spectra could not be assigned to particular phosphate residues in the oligonucleotide chain (Patel & Canuel, 1979; Gorenstein, 1981; Patel et al., 1982a,b, 1983a). The only exceptions, discussed further below, are the recently published data on the two d(CGCG) and d(TCGA) tetramers (Pardi et al., 1983; Petersheim et al., 1984).

† From the European Molecular Biology Laboratory, D-6900 Heidelberg, FRG (B.A.C.), and Max-Planck-Institut für experimentelle Medizin, Abteilung Chemie, D-3400 Göttingen, FRG (F.E.). *Received February 23, 1984.*

0006-2960/84/0423-5523$01.50/0